

Monte Carlo Hamiltonian: the Linear Potentials*

Xiang-Qian Luo, Jin-Jiang Liu, Chun-Qing Huang, Jun-Qin Jiang

Department of Physics, Zhongshan University, Guangzhou 510275, China

Helmut Kröger

Département de Physique, Université Laval, Québec, Québec G1K 7P4, Canada

November 13, 2002

Abstract

We further study the validity of the Monte Carlo Hamiltonian method. The advantage of the method, in comparison with the standard Monte Carlo Lagrangian approach, is its capability to study the excited states. We consider two quantum mechanical models: a symmetric one $V(x) = |x|/2$; and an asymmetric one $V(x) = \infty$, for $x < 0$ and $V(x) = x$, for $x \geq 0$. The results for the spectrum, wave functions and thermodynamical observables are in agreement with the analytical or Runge-Kutta calculations.

PACS numbers: 02.50.Ng, U, 03.65.-w, 03.65.Ge

Key words: Monte Carlo method, quantum mechanics, computational physics

Published in *Communications in Theoretical Physics* **38** (2002) 561-565.

*L.X.Q. is supported by the National Natural Science Fund for Distinguished Young Scholars, National Natural Science Foundation of China, Ministry of Education, Foundation of the Zhongshan University Advanced Research Center and Guangdong Provincial Natural Science Foundation. H.K. is support by NSERC Canada.

1 Introduction

Path integral quantization in the Lagrangian formulation and canonical quantization in the Hamiltonian formulation are two ways to quantize classical systems. Either one has advantages and disadvantages. The Lagrangian formulation is suitable for numerical simulations on a computer via Monte Carlo (MC). The enormous success of lattice gauge theory over the last two and half decades is certainly due to the fact that the MC method with importance sampling[1] is an excellent technique to compute high dimensional (and even “infinite” dimensional) integrals.

Unfortunately, using the Lagrangian formulation it is difficult to estimate wave functions and the spectrum of excited states. Wave functions in conjunction with the energy spectrum contain more physical information than the energy spectrum alone. Although lattice QCD simulations in the Lagrangian formulation give good estimates of the hadron masses, one is yet far from a comprehensive understanding of hadrons. Let us take as an example a new type of hadrons made of gluons, the so-called glueballs. Lattice QCD calculations[2] predict the mass of the lightest glueball with quantum number $J^{PC} = 0^{++}$, to be $1650 \pm 100 MeV$. Experimentally, there are at least two candidates: $f_0(1500)$ and $f_J(1710)$. The investigation of the glueball production and decays can certainly provide additional important information for experimental determination of a glueball. Therefore, it is important to be able to compute the glueball wave function.

In the Hamiltonian formulation, one can obtain the ground state energy, but also wave functions and the spectrum of excited states. Often, and in particular in the case of many-body systems, it is difficult to solve the stationary Schrödinger equation. Recently, we have suggested how to construct an effective Hamiltonian via MC[3] to describe the low energy spectrum and wave functions. The method has been tested in quantum mechanics[3, 4] in 1,2 and 3 spatial dimensions (the free system, the harmonic oscillator, the quartic potential, the local potential $V(x) = -V_0 \text{sech}^2(x)$) and the scalar model in quantum field theory[5] (Klein-Gordon model and ϕ^4 scalar model).

The purpose of this paper is to further test the viability of the MC Hamiltonian method in case of two potentials which generate a bound state spectrum:

$$V(x) = |x|/2, \tag{1}$$

and

$$V(x) = \begin{cases} \infty, & x < 0 \\ x, & x \geq 0. \end{cases} \tag{2}$$

These two models have their own interest in quantum theory. They have the form of a static quark-antiquark confining potential occurring in QCD. The second potential describes the particle moving above the surface of the ground. In our previous investigations, only symmetric potentials were considered. Here we would like to see if the method works for linear potentials and those with infinity and asymmetry.

The remainder of the paper is organized as follows. In Sect. 2, the basic ideas of the effective Hamiltonian method is briefly discussed. In Sect. 3, the numerical results are given. The conclusions are summarized in Sect. 4.

2 Effective Hamiltonian

The construction of an effective Hamiltonian starting from a regular basis in position space has been proposed in Ref. [3]. Following Feynman's path integral formulation [6], we consider the transition amplitude in imaginary time between time $t = 0$ and $t = T$. Using imaginary time makes the path integral mathematically well defined, and renders it amenable to numerical simulations by MC. Because the effective Hamiltonian is time independent, its construction in imaginary time should give the same result as in real time. We consider the transition amplitude for all combinations of positions $x_i, x_j \in \{x_1, \dots, x_N\}$,

$$M_{i,j}(T) = \langle x_i | e^{-HT/\hbar} | x_j \rangle = \int [dx] \exp[-S_E[x]/\hbar] \Big|_{x_j,0}^{x_i,T}, \quad (3)$$

where S_E denotes the Euclidean action. From the transition amplitudes $M_{ij}(T)$, one can construct the matrix

$$M(T) = [M_{i,j}(T)]_{N \times N}. \quad (4)$$

$M(T)$ is a positive, Hermitian and symmetric matrix. M can be factorized into a unitary matrix U and a real diagonal matrix $D(T)$, such that

$$M(T) = U^\dagger D(T) U. \quad (5)$$

Then from Eq.(3), Eq.(5) one can identify

$$U_{i,k}^\dagger = \langle x_i | E_k^{eff} \rangle, \quad D_k(T) = e^{-E_k^{eff} T/\hbar}. \quad (6)$$

The k -th eigenvector $|E_k^{eff}\rangle$ can be identified with the k -th column of matrix U^\dagger . The energy eigenvalues E_k^{eff} are obtained from the logarithm of the diagonal matrix elements of $D(T)$. This yields an effective Hamiltonian,

$$H_{eff} = \sum_{k=1}^N |E_k^{eff}\rangle \langle E_k^{eff}|. \quad (7)$$

We compute the matrix element $M_{i,j}(T)$ directly from the action via MC with importance sampling. For details see Ref.[3].

To get the correct scale for the spectrum, the position state $|x_k\rangle$ at initial time t_i or final time t_f (Bargman states or box states) should be properly normalized. We denote

a normalized basis of Hilbert states as $|e_k\rangle$, $k = 1, \dots, N$. In position space, it can be expressed as

$$e_k(x) = \begin{cases} 1/\sqrt{\Delta x_k}, & x \in [x_k, x_{k+1}] \\ 0, & x \notin [x_k, x_{k+1}] \end{cases} \quad (8)$$

where $\Delta x_k = x_{k+1} - x_k$. There is some arbitrariness in choosing a basis for the initial and final states. The simplest choice is a basis with $\Delta x_k = \text{const.}$, which is called the “regular basis”.

3 Numerical results

For the potential in Eq. (1) an exact solution of the ground state energy and wave function is analytically known [7]. They are given by

$$\begin{aligned} E_0^{Exact} &= \frac{|\xi_0|}{2}(\hbar^2/m)^{1/3} = 0.5094(\hbar^2/m)^{1/3}, \\ \psi_0(x) &= \sqrt{|\xi|} \left[J_{\frac{1}{3}}\left(\frac{2}{3}|\xi|^{3/2}\right) + J_{-\frac{1}{3}}\left(\frac{2}{3}|\xi|^{3/2}\right) \right], \end{aligned} \quad (9)$$

where $\xi = (|x| - 2E_0)(m/\hbar^2)^{1/3}$, $\xi_0 = \xi|_{x=0}$, $|\xi_0| = (3z_0/2)^{2/3}$, z_0 is the solution to the equation

$$J_{2/3}(z) - J_{-2/3}(z) = 0, \quad (10)$$

and $J_{1/3}$ and $J_{-1/3}$ are Airy functions. We compare two methods: the MC Hamiltonian method and the Runge-Kutta algorithm with the node theorem. The latter one means that we solve the stationary Schrödinger equation expressed as differential equation in position space and search for the discrete eigenvalue E_n corresponding to the number of nodes of the wave function. Here n denotes the quantum number, being related Eq. (7) to k by $n = k - 1$. Because the transition matrix is symmetric, we implement in the code

$$\begin{aligned} M_{i,j} &= (M_{i,j} + M_{j,i})/2, \\ M_{j,i} &= M_{i,j}, \end{aligned} \quad (11)$$

when calculating the matrix elements using the MC Hamiltonian method. There is an additional symmetry for the potential in Eq. (1): $V(-x) = V(x)$ so that the matrix elements should satisfy $M_{N+1-i, N+1-j} = M_{i,j}$. Therefore, in the code

$$\begin{aligned} M_{i,j} &= (M_{i,j} + M_{N+1-i, N+1-j})/2, \\ M_{N+1-i, N+1-j} &= M_{i,j}. \end{aligned} \quad (12)$$

n	E_n^{Exact}	$E_n^{R.K.}$	E_n^{MC}	$\Delta E_n^{MC}/E_n^{R.K.}$
0	0.509	0.509	0.504 ± 0.002	1.0%
1		1.169	1.171 ± 0.002	0.2%
2		1.624	1.622 ± 0.002	0.1%
3		2.044	2.047 ± 0.003	0.2%
4		2.410	2.407 ± 0.004	0.1%
5		2.760	2.764 ± 0.007	0.1%
6		3.082	3.075 ± 0.021	0.2%
7		3.393	3.399 ± 0.034	0.2%
8		3.686	3.669 ± 0.078	0.5%
9		3.972	3.982 ± 0.019	0.3%
10		4.244	4.202 ± 0.105	1.0%
11		4.511	4.532 ± 0.041	0.5%
12		4.768	4.683 ± 0.069	1.8%
13		5.020	5.074 ± 0.142	1.0%
14		5.264	5.155 ± 0.153	2.1%
15		5.504	5.673 ± 0.137	3.1%
16		5.738	5.708 ± 0.117	0.5%

Table 1: Spectrum corresponding to the potential in Eq. (1). Here E_n^{Exact} , $E_n^{R.K.}$ and $E_n^{M.C.}$ denote respectively the data from the analytic solution, Runge-Kutta algorithm and MC Hamiltonian. The input parameters are $m = 1$, $\hbar = 1$, $\Delta x = 1$ and $N = 21$. The statistical an relative errors of E_n^{MC} are also shown. The error of the Runge-Kutta algorithm is less than the last digit and not shown.

The use of these symmetries lead to reduction of the numerical errors. We have computed the energy spectrum, wave functions as well as thermodynamical observables such as average energy, specific heat and the partition function. The results can be summarized as follows. Fig. 1 shows the ground state wave function. One observes good agreement between the MC Hamiltonian result and the exact solution. Fig. 2 shows a similar comparison for the wave function of the first excited state. Tab. 1 shows the data for the spectrum.

The model described by the potential in Eq. (2) is exactly solvable. The spectrum and wave function are given by

$$\begin{aligned}
E_n &= \lambda_n (\hbar^2/2m)^{1/3}, \\
\psi_n(x) &= \begin{cases} 0, & x < 0 \\ \sqrt{|\xi_n|} \left[J_{\frac{1}{3}}\left(\frac{2}{3}|\xi|^{3/2}\right) + J_{-\frac{1}{3}}\left(\frac{2}{3}|\xi|^{3/2}\right) \right], & x \geq 0, \end{cases}
\end{aligned} \tag{13}$$

n	E_n^{Exact}	E_n^{MC}	$\Delta E_n^{MC}/E_n^{Exact}$
0	1.856	1.774 ± 0.086	4.4 %
1	3.244	3.182 ± 0.112	1.9 %
2	4.382	4.346 ± 0.125	0.8 %
3	5.383	5.300 ± 0.082	1.6 %

Table 2: Spectrum corresponding to the potential in Eq. (2). The input parameters are $m = 1$, $\hbar = 1$, $\Delta x = 1$ and $N = 20$.

where $\xi_n = (x - E_n) \left(2m/\hbar^2\right)^{1/3}$, and λ_n is the solution to the equation

$$J_{\frac{1}{3}}\left(\frac{2}{3}|\lambda_n|^{3/2}\right) + J_{-\frac{1}{3}}\left(\frac{2}{3}|\lambda_n|^{3/2}\right) = 0. \quad (14)$$

Here are the first few: $\lambda_0 = 2.338$, $\lambda_1 = 4.088$, $\lambda_2 = 5.521$ and $\lambda_3 = 6.787$. Fig. 3, Fig. 4 and Tab.2 show a comparison of the spectrum and wave functions corresponding to the potential in Eq. (2). Although the agreement is good, the relative errors are bigger, in comparison with the first case. This might be due to the lack of parity symmetry in the potential Eq. (2).

The partition function is defined by $Z(\beta) = Tr(e^{-\beta H})$. The average energy is defined by $U(\beta) = Tr(He^{-\beta H})/Z$, and the specific heat by $C(\beta) = \partial U/\partial \tau$. We have used the following notation: $\beta = (k_B \tau)^{-1}$, τ is the temperature, k_B is the Boltzmann constant, and we identify β with the imaginary time T by $\beta = T/\hbar$. Since we have approximated H by H_{eff} , we can express those thermodynamical observables via the eigenvalues of the effective Hamiltonian

$$\begin{aligned} Z^{\text{eff}}(\beta) &= \sum_{k=1}^N e^{-\beta E_k^{\text{eff}}}, \\ U^{\text{eff}}(\beta) &= \sum_{k=1}^N \frac{E_k^{\text{eff}} e^{-\beta E_k^{\text{eff}}}}{Z^{\text{eff}}(\beta)}, \\ C^{\text{eff}}(\beta) &= k_B \beta^2 \left(\sum_{k=1}^N \frac{(E_k^{\text{eff}})^2 e^{-\beta E_k^{\text{eff}}}}{Z^{\text{eff}}(\beta)} - (U^{\text{eff}}(\beta))^2 \right). \end{aligned} \quad (15)$$

The numerical results are shown in Fig.5 to Fig. 8. One observes good agreement between the results from the MC Hamiltonian and the reference solution.

4 Conclusion

In the preceding sections, we have applied the MC Hamiltonian method[3] to the linear potentials: one is symmetric, and another is asymmetric and has infinity. The results for

the spectra, wave functions and thermodynamical observables are in good agreement with other methods. We also observe that the use of the parity symmetry whenever exists, can lead to systematic reduction of numerical errors.

In most cases, where no exact solution is available, numerical solution is required. Runge-Kutta method works only in 1D and it is very difficult to obtain information on the excited states by standard Lagrangian MC approach. In our opinion, the MC Hamiltonian has an advantage in these cases.

The MC Hamiltonian method approximates a quantum system with infinite states by a finite system with dimension N . Increasing N , we can obtain more excited states, and reduce the systematic errors. Larger N value is also necessary when approaching the smaller β (or higher temperature regime). However, the computation of the matrix elements is very time consuming. In this paper, we used the regular basis, which is good enough for few body quantum mechanics and might not be very efficient for quantum field theory. In Ref. [5], we suggested the concept of MC Hamiltonian using the stochastic basis and applied it successfully to the Klein-Gordon model and ϕ^4 scalar model. We believe that the application to more complicated systems will be very interesting.

References

- [1] N. Metropolis, A. Rosenbluth, M. Rosenbluth, A. Teller and E. Teller, J. Chem. Phys. **21** (1953) 1087.
- [2] X.Q. LUO and Q. CHEN, Mod. Phys. Lett. **A11** (1996) 2435;
X.Q. LUO, Q. CHEN, S. GUO, X. FANG and J. LIU, Nucl. Phys. **B(Proc. Suppl.)53** (1997) 243.
- [3] H. Jirari, H. Kröger, X.Q. LUO and K. Moriarty, Phys. Lett. **A258** (1999) 6.
- [4] X.Q. LUO, J. Jiang, C. HUANG, H. Jirari, H. Kröger, and K. Moriarty, Nucl. Phys. **B(Proc. Suppl.)83** (2000) 810.
H. Jirari, H. Kröger, C. HUANG, J. JIANG, X.Q. LUO, and K. Moriarty, Nucl. Phys. **B(Proc. Suppl.)83** (2000) 953.
X.Q. LUO, C. HUANG, J. JIANG, H. Jirari, H. Kröger, K. Moriarty, Physica A281 (2000) 201;
C. HUANG, J. JIANG, X.Q. LUO, H. Jirari, H. Kröger, and K. Moriarty, High Energy Phys. Nucl. Phys. 24 (2000) 478;
J. JIANG, C. HUANG, X.Q. LUO, H. Jirari, H. Kröger, and K.J.M. Moriarty, Commun. Theor. Phys. **34** (2000) 723;
X. Q. LUO, H. XU, J. YANG, Y. WANG, D. CHANG, Y. LIN, and H. Kröger, Commun. Theor. Phys. **36** (2001) 7.

- [5] C. HUANG, H. Kröger, X.Q. LUO, and K. Moriarty, Phys. Lett. A **299** (2002) 483;
X.Q. LUO, H. Jirari, H. Kröger, and K. Moriarty, in Non-perturbative Methods and
Lattice QCD, X.Q. LUO and E. Gregory eds., World Scientific, Singapore (2001)
100.
X.Q. LUO, H. Jirari, H. Kröger, and K. Moriarty, in Advanced Computing and
Analysis Techniques in Physics Research: VII International Workshop; ACAT 2000,
American Institute of Physics (2001) 217.
- [6] R.P. Feynman and A.R. Hibbs, Quantum Mechanics and Path Integrals, McGraw-
Hill, New York (1965).
- [7] B.C. QIAN and J.Y. ZENG, Selected Exercises and Analysis in Quantum Mechanics,
Science Publisher, Beijing (1988), p.470.

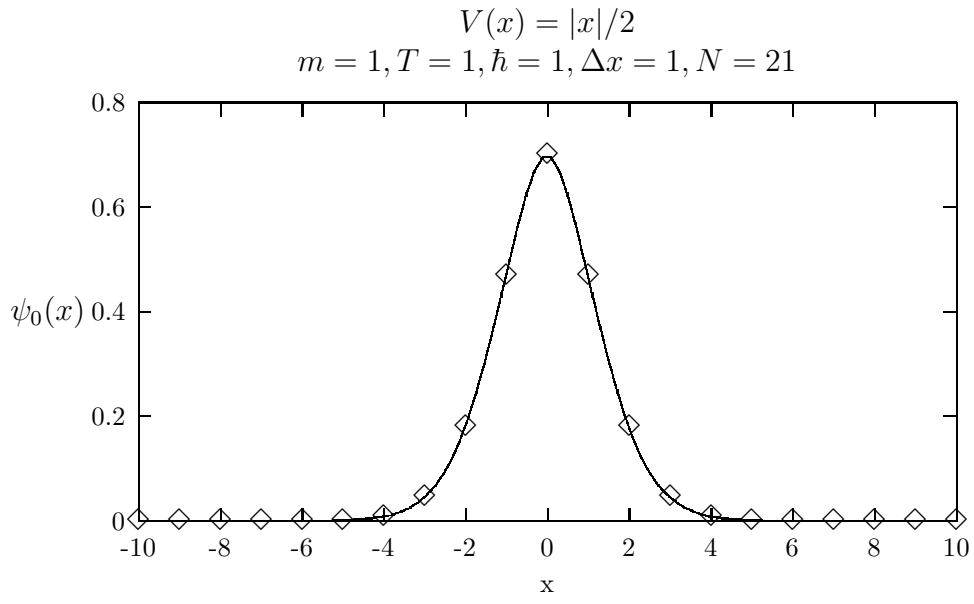


Figure 1: Ground state wave function $\psi_0(x)$ corresponding to the potential in Eq. (1), where the continuous line represents the result from the Runge-Kutta method and the symbols stand for the data from the MC Hamiltonian method.

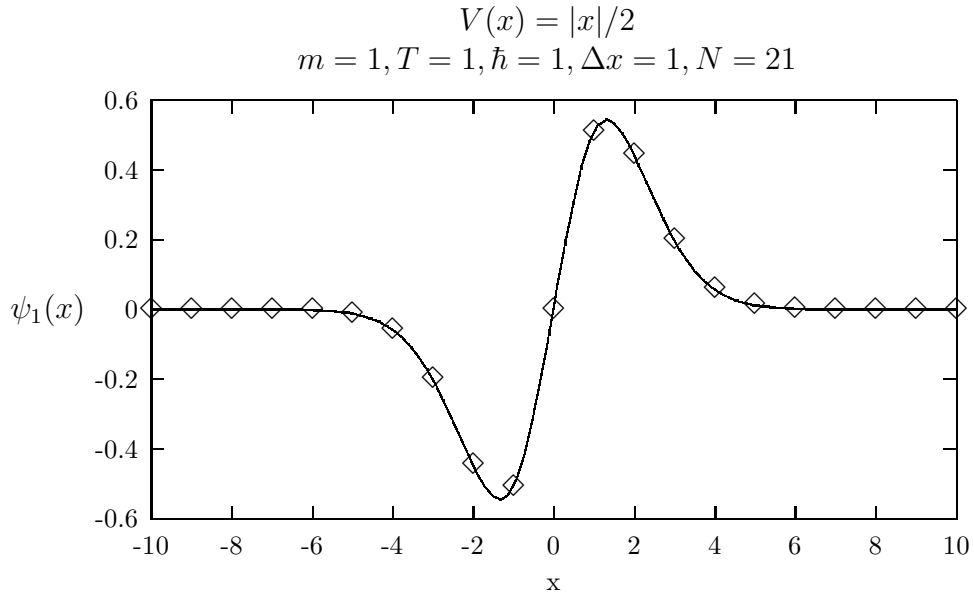


Figure 2: Same as Fig. 1, but for first excited state $\psi_1(x)$.

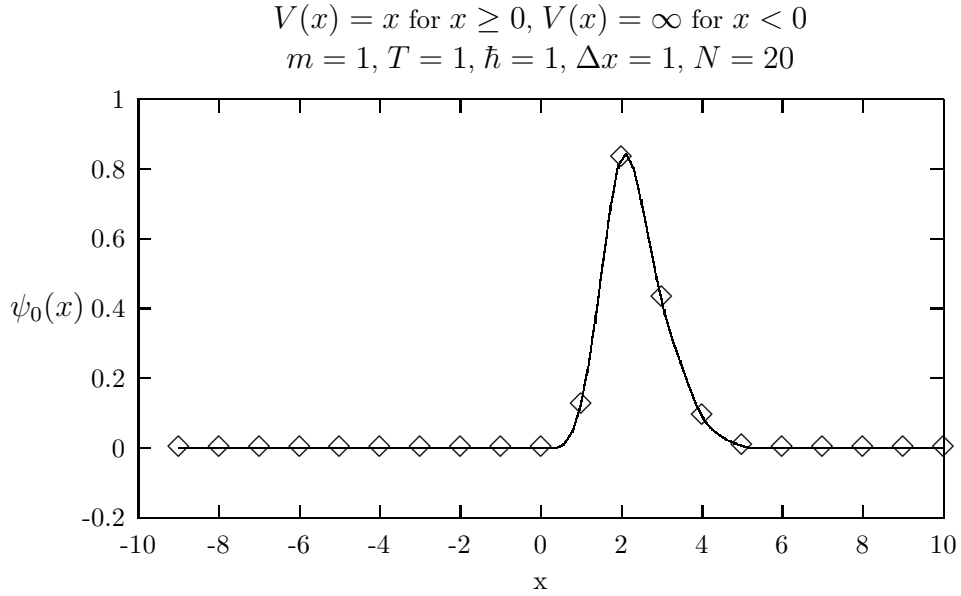


Figure 3: Ground state wave function $\psi_0(x)$ corresponding to the potential in Eq. (2), where the continuous line represents the exact solution and the symbols stand for the data from the MC Hamiltonian method.

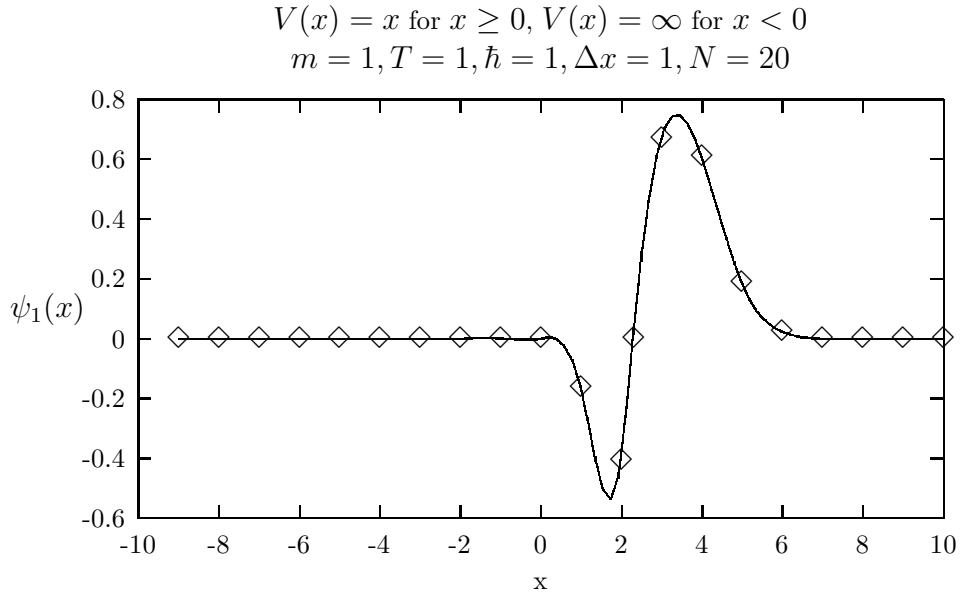


Figure 4: Same as Fig. 3, but for first excited state $\psi_1(x)$.

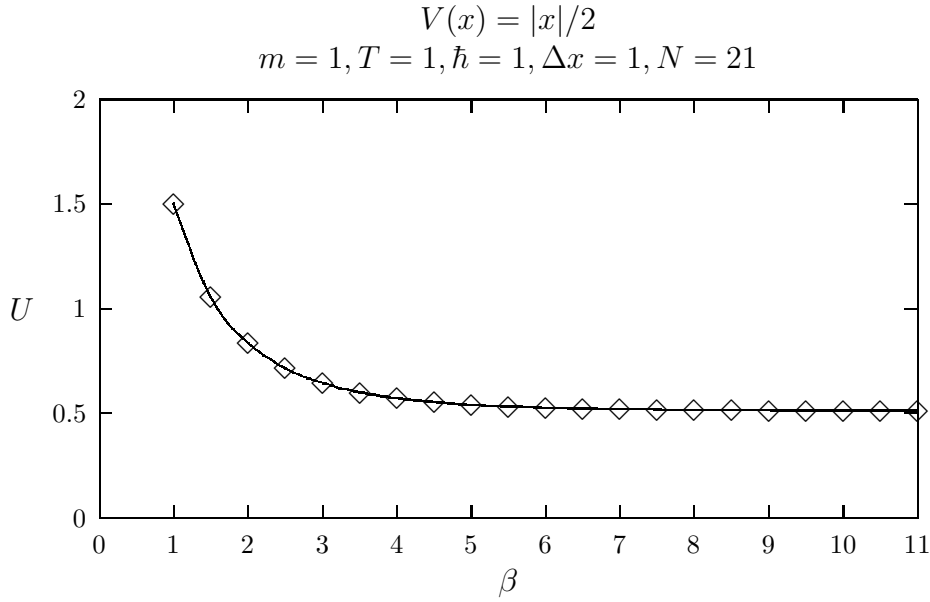


Figure 5: Average energy $U(\beta)$ corresponding to the potential in Eq. (1), where the continuous line represents the result obtained by substituting the eigenvalues of the Runge-Kutta method into Eq. (15) and the symbols stand for the data from the MC Hamiltonian method.

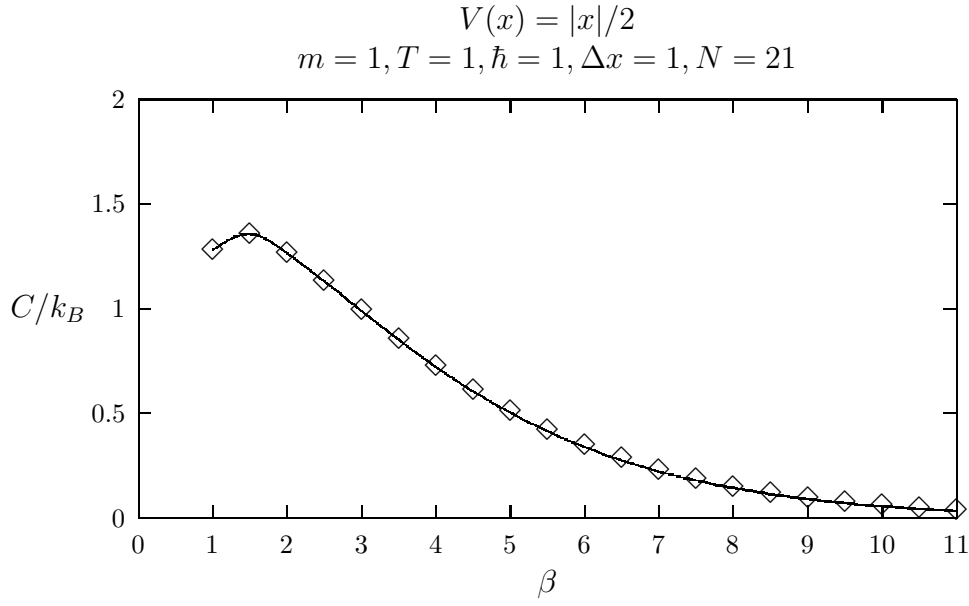


Figure 6: Same as Fig. 4, but for specific heat $C(\beta)$.

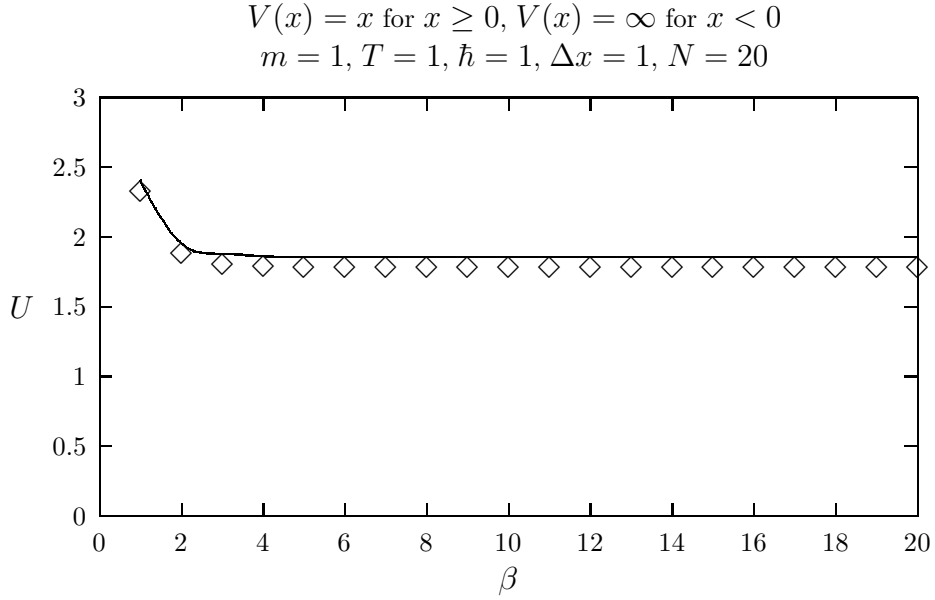


Figure 7: Average energy $U(\beta)$ corresponding to the potential in Eq. (2), where the continuous line represents the result obtained by substituting the eigenvalues of the analytic solution into Eq. (15) and the symbols stand for the data from the MC Hamiltonian method.

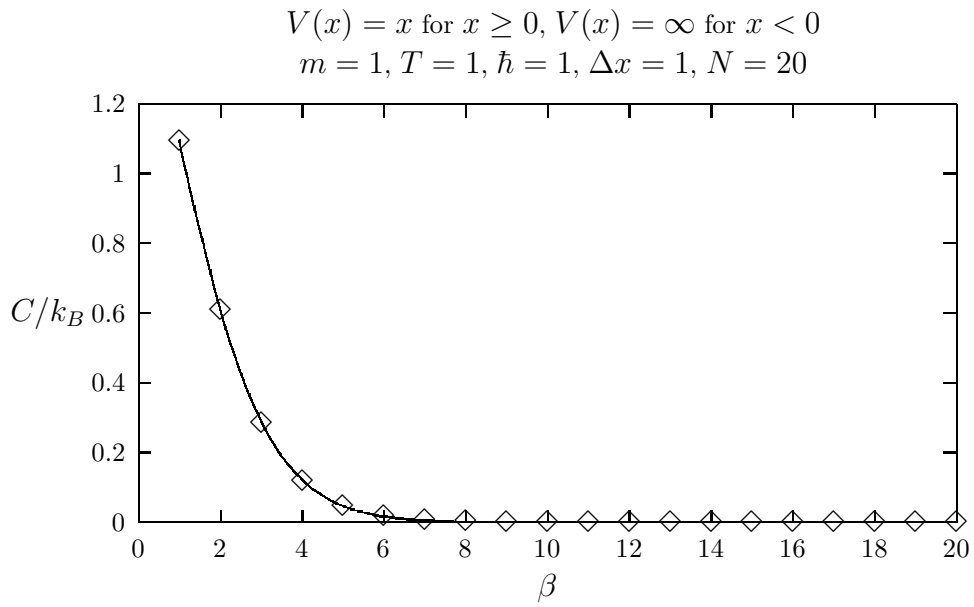


Figure 8: Same as Fig. 7, but for specific heat $C(\beta)$.